

- (25) A. D. Allen, F. Bottomley, R. A. Harris, V. P. Reinsalu, and C. V. Senoff, *J. Am. Chem. Soc.*, **89**, 5595 (1967).  
 (26) R. Gagne, C. Koval, and T. Smith, Abstracts, 174th National Meeting of the American Chemical Society, Chicago, Ill., Aug 1977, No. INOR-85.  
 (27) In terms of eq 7, this is the same as saying that the effective dielectric

constant of the solvent,  $D_{\text{eff}}$ , is better approximated by the infinite frequency dielectric constant,  $D_{\infty}$ , which measures the polarizability of the solvent, than by the static dielectric constant  $D$ , which also includes effects caused by the motion of solvent dipoles due to molecular tumbling. Note that  $D_{\infty} \approx n^2$ .

## The Molybdenum Site of Nitrogenase. 2. A Comparative Study of Mo-Fe Proteins and the Iron-Molybdenum Cofactor by X-Ray Absorption Spectroscopy

Stephen P. Cramer,<sup>1a</sup> William O. Gillum,<sup>1a</sup> Keith O. Hodgson,\*<sup>1a</sup>  
 Leonard E. Mortenson,<sup>1b</sup> Edward I. Stiefel,<sup>1c</sup> John R. Chisnell,<sup>1d</sup> Winston J. Brill,<sup>1d</sup>  
 and Vinod K. Shah<sup>1d</sup>

Contribution from the Department of Chemistry, Stanford University, Stanford, California 94305, Department of Biological Sciences, Purdue University, West Lafayette, Indiana 47907, Charles F. Kettering Research Laboratory, Yellow Springs, Ohio 45387, and Department of Bacteriology and Center for Studies of Nitrogen Fixation, University of Wisconsin, Madison, Wisconsin 53706.  
 Received December 1, 1977

**Abstract:** Recently, the Mo environment in lyophilized MoFe protein from *Clostridium pasteurianum* has been structurally characterized by x-ray absorption spectroscopy measurements. As a further step in elucidating the structure and relationship of the Mo environment in other species, the MoFe component from *Azotobacter vinelandii* has been studied. The K-edge Mo x-ray absorption spectra for the intact crystalline MoFe component and for the cofactor (FeMo-co) derived from this component have been recorded. There exists a striking similarity in both the edge and EXAFS regions of the spectra between the *Clostridium* and *Azotobacter* data. Detailed analysis leads to the conclusion that the Mo environment is not significantly perturbed by the lyophilization process and that the Mo environment in the protein from *Azotobacter* has the same environment at the Mo site—an as yet chemically unknown Mo-Fe-S cluster. Finally, the studies show that the basic features of the Mo environment in the cofactor are preserved during the extraction process and that the intact protein and the cofactor share quite similar Mo sites. These data lend quantitative support to the idea of a common Mo site in the nitrogenase MoFe proteins.

### Introduction

Because of its spectroscopic obscurity, virtually nothing has been known until recently about the molybdenum site in the nitrogenase Mo-Fe protein (also known as component I).<sup>2a</sup> As a first step in the application of x-ray absorption spectroscopy<sup>2b</sup> to the study of molybdenum in nitrogenase, the x-ray absorption spectrum of lyophilized, semireduced *Clostridium pasteurianum* Mo-Fe protein (Cpl) was recorded and analyzed.<sup>3</sup> Furthermore, the absorption edge region spectra for this protein in the fully reduced, semireduced, dye-oxidized, and air-oxidized states were obtained and compared with edges of known Mo structures.<sup>3</sup> The combined edge and EXAFS data were interpreted as evidence for a primarily sulfur, non-Mo=O nitrogenase Mo environment, and the EXAFS itself was best explained by postulating a Mo, Fe, S cluster.<sup>3</sup>

Considering the novelty of the spectroscopic techniques involved, the air sensitivity of the nitrogenase enzyme, and the importance of the structural conclusions, it appeared important to reproduce the results of the Cpl investigation on another bacterial nitrogenase. Accordingly, x-ray absorption spectra have been obtained for the *Azotobacter vinelandii* nitrogenase Mo-Fe protein (Avl) and for the iron-molybdenum cofactor (FeMo-co) isolated from Avl.<sup>4</sup> The Avl and FeMo-co spectra are quite similar to those previously obtained on Cpl, indicating similar molybdenum environments in all three samples. These results therefore reinforce the previous Mo, Fe, S cluster hypothesis initially proposed on the basis of the Cpl data.<sup>3</sup> The Avl spectra demonstrate that useful EXAFS data can be obtained on the Mo-Fe protein under aqueous conditions, thereby making possible a variety of interesting experiments. Fur-

thermore, although the current FeMo-co spectra are of lower quality than the intact protein spectra, it has been verified that the cofactor preserves the essential features of the nitrogenase Mo site. Further study of this material at higher concentrations should yield a wealth of detailed structural information about the metal sites of nitrogenase.

### Experimental Section

**Avl Preparation and Handling.** The Avl protein was prepared at the Charles F. Kettering Research Laboratory (CFKRL) by modifications of procedures due to Bulen and LeComte<sup>5a</sup> and Shah and Brill.<sup>6</sup> In this procedure the final step involves crystallization in 0.046 M NaCl in Tris buffer (pH 7.4) at 38 °C. The precipitated crystals were washed with 0.046 M NaCl in 0.025 M Tris buffer (pH 7.4) containing 1 mg/mL Na<sub>2</sub>S<sub>2</sub>O<sub>4</sub> and centrifuged anaerobically at 12 000 g for 10 min to yield a soft pellet. The sealed centrifuge tube was taken into an argon-filled Vacuum Atmospheres box where a gas-tight syringe was used with a 16-gauge cannula to transfer the paste from the centrifuge tube to the Lucite sample cell. The sealed cell was frozen in dry ice and kept at dry ice temperatures throughout shipment and data collection until returned to CFKRL for analysis. The cell was opened in the argon-filled box and the protein dissolved in 0.25 M NaCl in 0.025 M Tris buffer (pH 7.4). It was then analyzed in parallel with a small amount of sample from the same preparation which had been stored in liquid N<sub>2</sub>.

The unirradiated protein had a specific activity of 1300 nmol C<sub>2</sub>H<sub>4</sub> min<sup>-1</sup> mg<sup>-1</sup> of protein while that which had been subject to x-ray spectroscopy had an activity of 1100 nmol C<sub>2</sub>H<sub>4</sub> min<sup>-1</sup> mg<sup>-1</sup> protein. Polyacrylamide gel electrophoreses, loaded with 90 μg of protein on 5-mm diameter cylindrical gels, were identical for the two samples, showing a single large band when stained with Coomassie brilliant blue and a very faint trailing band which is not visible in photographs of the gels. The EXAFS sample contained 6.2 nmol of Mo and 102

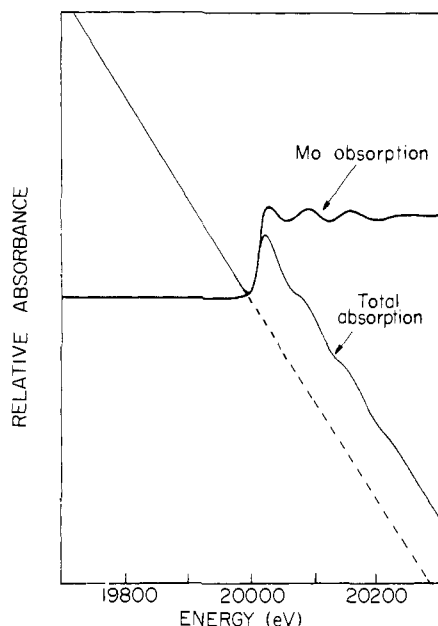


**Figure 1.** The pre-edge extrapolation and subtraction procedure used to separate the Mo component of the x-ray absorption from the protein and solvent background. A curve of the form  $A_{\text{preedge}} = c_0 + c_1E + c_2E^{-1}$  (where  $E$  is the photon energy and  $A_{\text{preedge}}$  is the total absorption before the Mo edge) was fitted to the total absorption spectrum on the range of 19 600–19 950 eV. Extrapolation and subtraction of this curve beyond the Mo K edge yielded a residual curve representing the Mo K edge component of the total absorption, which was then used to calibrate the EXAFS amplitude.

nmol of Fe/mg protein. There were 206 mg of protein and 1.3  $\mu\text{mol}$  of Mo in about 0.75 mL volume of paste in the cell. Protein was determined by the biuret method;<sup>5b</sup> Mo was determined by the Bulen and LeComte<sup>5a</sup> modification of the Clark and Axley procedure;<sup>5c</sup> and Fe was determined by the bathophenanthroline method of Peterson.<sup>5d</sup>

**FeMo-co Preparation and Handling.** FeMo-co was isolated from crystalline Mo-Fe protein of *A. vinelandii* nitrogenase by the method of Shah and Brill.<sup>4</sup> Approximately 100 mg of crystalline Mo-Fe protein was used for the preparation of FeMo-co and the concentrated fractions were evaporated to dryness at room temperature using a diffusion pump. The residue was dissolved in about 1.0 mL of NMF containing 1.2 mM sodium dithionite and 5 mM  $\text{Na}_2\text{HPO}_4$  and loaded into the Lucite cell through a port fitted with a rubber septum. All operations were carried out under a  $\text{H}_2$  atmosphere. After the sample was loaded in the Lucite cell, a piece of Lucite was glued in place over the port to minimize  $\text{O}_2$  diffusion. The cuvette was immediately placed in dry ice and kept near dry ice temperature throughout shipment and data collection.

Upon return of the sample to Wisconsin, a small hole was drilled in the Lucite piece covering the rubber stopper and the sample was transferred with a syringe to an anaerobic vial fitted with a serum stopper. This solution of FeMo-co, when assayed by activation of inactive Mo-Fe protein in *A. vinelandii* mutant strain UW45, had an activity of 176  $\mu\text{mol}$  ethylene formed  $\text{min}^{-1} \text{mL}^{-1}$ . This sample, assayed before x-ray absorption, had an activity of 200  $\mu\text{mol}$  ethylene formed  $\text{min}^{-1} \text{mL}^{-1}$  (88% recovery). The FeMo-co preparation had 470 nmol of molybdenum/mL.

**Data Collection and Analysis.** The spectra were recorded at dry ice temperature at the Stanford Synchrotron Radiation Laboratory as described previously.<sup>3</sup> The EXAFS analysis procedure has been presented in an earlier paper on molybdenum complexes of known structure,<sup>2b</sup> and the details of the numerical analysis programs have also been described.<sup>7</sup>

Because the molybdenum concentrations in the Avl and FeMo-co samples were relatively low, compared to the previous lyophilized Cpl sample, EXAFS data collection was pressing the capabilities of the instrument. The absorption due to Mo was on the order of 5% of the total x-ray absorption for the Avl sample, and even less for the FeMo-co. Isolation of the Mo absorption component was accomplished by extrapolation and subtraction of a "preedge" function fitted

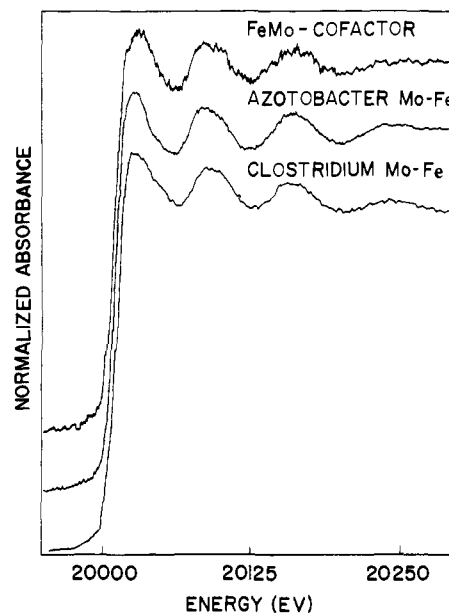


**Figure 2.** A comparison of the Mo absorption components of lyophilized Cpl (bottom), crystallized Avl (middle), and NMF-extracted FeMo-co (top).

to the data below the Mo K edge, as illustrated in Figure 1. The EXAFS itself was removed from the total absorption through use of a cubic spline fitting procedure<sup>7</sup> and normalized relative to the Mo absorption component.

## Results

In Figure 2, the Mo components of the x-ray absorption spectra of Cpl, Avl, and FeMo-co are presented. Following the absorption edge peak at about 20 030 eV, there are two distinct maxima near 20 090 and 20 160 eV. Another weak peak at 20 240 eV is evident in the Cpl and Avl spectra; this feature may be obscured by noise in the FeMo-co data. Thus, at this level of comparison, the spectra for all three samples are very similar. Since the data reflect only the molybdenum environments of these substances, one can therefore conclude that molybdenum retains essentially the same type of ligands and similar bond lengths in Cpl, Avl, and FeMo-co. However, such a visual comparison of similar features in the absorption spectra is only the preliminary stage in the interpretation of these data. In order to make further quantitative estimates of the molybdenum site similarity, these spectra have been subjected to a detailed numerical analysis.

At this point, because of the different types of electronic transitions involved, it is convenient to divide the spectra into two regions. The edge region, from approximately 20 000 to 20 050 eV, will be discussed first. At the low end of this energy range, the Mo absorption is due to transitions of the Mo 1s electron to molecular orbitals of primarily metal character, while at higher energies transitions to quasi-bound states and the continuum begin. Analysis of the shape and position of the absorption edge region can reveal details of the metal site symmetry, oxidation state, and the nature of the surrounding ligands.<sup>8-10</sup>

The second part of the analysis will involve the EXAFS region (from just beyond the absorption edge region to as far out as the data permit). The features in this region arise from transitions in which the outgoing photoelectron wave is backscattered by atoms in the vicinity (out to about 3–5 Å) of the absorber. We have previously described in detail how analysis of the EXAFS can provide information about the number, type, and distances of atoms in the first, and sometimes second, molybdenum coordination spheres.<sup>2b</sup> The combined studies of both edge and EXAFS data can then be

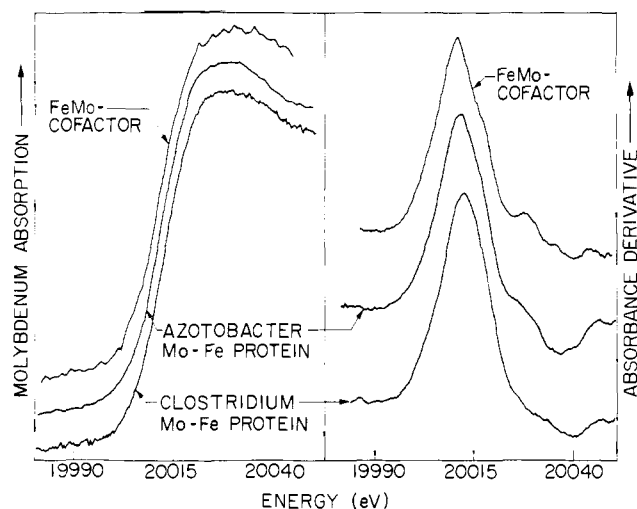


**Figure 3.** A comparison of the Mo absorption edge regions of Cpl, Avl, and FeMo-co. The Cpl data are an average of solution and lyophilized spectra.

used to make some specific conclusions about the nitrogenase molybdenum environment.

**The Absorption Edge Region.** The Mo K x-ray absorption edges for Cpl, Avl, and FeMo-co in their "as-isolated" (semi-reduced) states are presented in Figure 3. As discussed previously,<sup>3</sup> the position of the Cpl edge inflection point,  $20\,011.7 \pm 1$  eV, is in a region characteristic of molybdenum with sulfur ligation. The new data show that the Avl and FeMo-co edges are in the same region,  $20\,010.7$  and  $20\,010.6$  eV, respectively. Within experimental error, all three of these edges have the same inflection point energy. It thus appears that the same high-sulfur molybdenum environment is present in all three cases.

The shapes of these three edges, best revealed by the derivative curves on the right-hand side of Figure 3, are also extremely similar. It was noted previously<sup>3,8</sup> that the presence of doubly bound oxygen ( $\text{Mo}=\text{O}$ ) or tetrahedral geometry is invariably linked with a two inflection point absorption edge. The extra low energy inflection point is caused by the addition of a broad Lorentzian-shaped  $1s-4d$  transition to the smoothly rising absorption edge; these effects are discussed in detail in ref 3. However, all three edges of Figure 3 have only a single inflection point in the vicinity of  $20\,011$  eV. The weakness of the  $1s-4d$  transition in these cases allows one to rule out  $\text{Mo}=\text{O}$  coordination and tetrahedral geometry for molybdenum in Avl and FeMo-co, as was done previously for Cpl.<sup>3</sup> Furthermore, the similarity in the shape and position of all three edges makes it extremely unlikely that more than two ligands are different between these three cases. In fact, postulation of identical molybdenum environments is reasonable based on the absorption edge data alone.

**The EXAFS Region.** The EXAFS of lyophilized Cpl, crystallized Avl, and FeMo-co in a solution of *N*-methylformamide (NMF) are presented in Figure 4. On the range of  $3-7 \text{ \AA}^{-1}$  the phases of all three spectra are almost identical; furthermore, they all show a distinct beat pattern in the amplitude envelope with a maximum near  $6 \text{ \AA}^{-1}$  and a minimum near  $9.5 \text{ \AA}^{-1}$ . Although they exhibit less correspondence near the beat minimum from  $9$  to  $10.5 \text{ \AA}^{-1}$ , the Avl and Cpl spectra also show similar peaks and troughs at about  $11.2$  and  $12.0 \text{ \AA}^{-1}$ , respectively.

The fact that the spectra are clearly in phase until at least  $7 \text{ \AA}^{-1}$  indicates that not only are the distances from molybdenum to neighboring atoms similar, but that the same elemental types of atoms are present as well. In the previous analysis of the Cpl data,<sup>3</sup> the strongest EXAFS component was

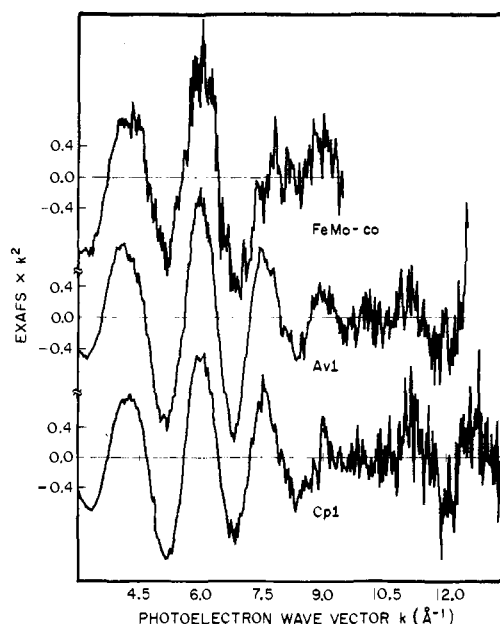


**Figure 4.** A comparison of the EXAFS of Cpl, Avl, and FeMo-co. The  $E_0$  used for defining  $k$  was  $20\,025$  eV for all spectra.

assigned to a Mo-S interaction. If mostly oxygen ligands were present instead of mostly sulfur ligands in any of these cases, the spectra would be out of phase with the current data. Thus, even if the Mo-O distances were the same as the Mo-S distances, the locations of the peaks and troughs in the spectra would be reversed. This is because of the difference between the phase shifts (about  $3.5$  rad) for oxygen and sulfur, as illustrated in Figures 5 and 13 of ref 2b. Thus, in agreement with the absorption edge data, the EXAFS indicates that molybdenum is surrounded primarily or completely by sulfur ligands in all three cases.

The fact that all three spectra exhibit a beat pattern in the amplitude envelope is supportive of the existence of a second EXAFS component, indicating a second Mo-scatterer distance which must be accounted for. Such beat patterns occur when two absorber-scatterer interactions of comparable magnitude are present; simple examples are illustrated in Figure 7 of ref 2b. The second EXAFS component was tentatively identified as a Mo-Fe interaction in the earlier Cpl analysis,<sup>3</sup> and the existence of some form of a Mo, Fe, S cluster was proposed. Although the current cofactor data are not good enough to prove the presence of such a cluster, the spectral correspondence with the intact protein EXAFS allows one to conclude that the Mo environment after the NMF extraction procedure is very similar to that of the native protein.

Since the FeMo-co data are substantially noisier than the Avl or Cpl spectra, it is presently impossible to say whether the discrepancy in the vicinity of  $k = 7.5 \text{ \AA}^{-1}$  is real or artifactual. An estimate of possible structural differences can be made by assuming that the FeMo-co EXAFS is  $\pi/2$  out of phase with the intact Mo-Fe protein spectra at  $7.5 \text{ \AA}^{-1}$ , and that this mismatch is caused by a change in a single set of Mo-S distances. Then since  $2k(R_{\text{Mo-S}}(\text{protein}) - R_{\text{Mo-S}}(\text{cofactor})) \approx \pi/2$ , the difference in Mo-S distances can be no more than about  $0.1 \text{ \AA}$ . In summary, a similar molybdenum structural unit appears to be present in FeMo-co and in the intact proteins, and even with rather limited data the similarity in average Mo-S distances can be confirmed to about  $0.1 \text{ \AA}$ .

Because the Avl data are useful over a wider range in  $k$  space, a more detailed comparison with the Cpl EXAFS is possible. One means of comparing the EXAFS frequency components is through Fourier transformation, and the Fourier transforms of the Avl and Cpl data are compared in Figure 5.

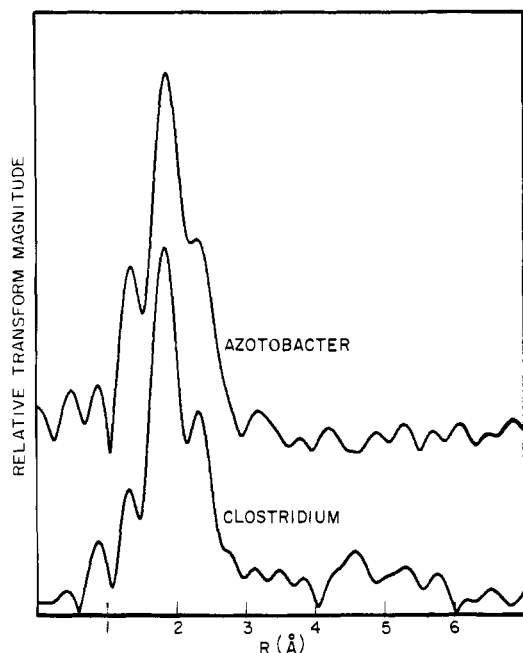


**Figure 5.** A comparison of the Fourier transform magnitudes for the Avl and Cpl EXAFS. Transform range: 4–12.5  $\text{\AA}^{-1}$ ,  $k^3$  expansion.

The use of the Fourier transform to interpret EXAFS data has been explained previously.<sup>2b,11</sup> Using a  $k^3\chi(k)$  transform on the range of 4–12.5  $\text{\AA}^{-1}$ , Cpl and Avl transforms exhibit major peaks at 1.84 and 1.87  $\text{\AA}$ , respectively, with secondary peaks at 2.32 and 2.31  $\text{\AA}$ , and a third feature at lower  $R$  values. When the appropriate phase shifts are applied, the major peak corresponds to an average Mo–S distance of 2.35  $\text{\AA}$  in Avl and 2.32  $\text{\AA}$  in Cpl. The high  $R$  peak transform was previously interpreted as a Mo–Fe interaction at 2.72  $\text{\AA}$  in the Cpl analysis,<sup>3</sup> and the same interpretation of the Avl transform appears reasonable. The low  $R$  feature in the Cpl transform was considered to be a mathematical artifact, but this feature is too large to easily dismiss in the Avl data.

A persistent problem in the interpretation and quantitative analysis of EXAFS data has been the ambiguity in correctly removing the residual background absorption component from the oscillatory EXAFS component. This problem of “background subtraction” is especially severe in dealing with dilute sample spectra in which the absorption component of interest is only a few percent of the total absorption. In such cases, the magnitude of the EXAFS is less than 1% of the total absorption. Small discrepancies between the true background and the cubic spline polynomial used to fit this background will produce low-frequency artifacts in the derived EXAFS spectrum. Although Fourier filtering procedures are sometimes useful for removing the lowest frequency components of residual background, they are not successful when the residual has frequency components near those of the “true” EXAFS, since “background” and “true” EXAFS are then mathematically indistinguishable.

The only way to decide whether the low-frequency component of the Avl EXAFS is real or an artifact will be to collect another spectrum under different conditions. Because of the time delay involved in such a task, the current data have been analyzed in two different ways. In one analysis the low-frequency component was presumed real and included within the range of the Fourier filter, while in the other case the low-frequency peak was excluded. A comparison of the resultant Fourier filtered Avl EXAFS, with each other and with the Cpl data, is presented in Figure 6. This comparison shows that the chief result of removing the low-frequency component is modification of the EXAFS near the beat minimum around

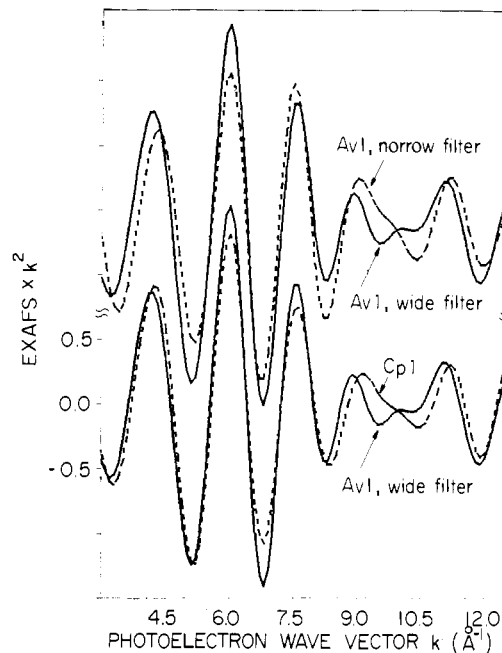


**Figure 6.** A comparison of the Fourier-filtered Avl and Cpl data. Top curves, (—) Avl EXAFS with low  $R$  peak included in filter, (---) Avl data with low  $R$  peak partially excluded by filter. Bottom curves, (—) Avl data with low  $R$  peak included in filter, (---) Cpl data with low  $R$  peak included in filter. Note good match at all points except in region of beat minimum.

10  $\text{\AA}^{-1}$ . Both of these alternate Fourier-filtered Avl EXAFS data sets were analyzed by the same curve-fitting procedure used to interpret the Cpl EXAFS.<sup>3</sup>

General principles for the curve fitting of EXAFS spectra are summarized in ref 2b. One procedure is to postulate a given set of atoms around the x-ray absorbing atom, and to vary parameters corresponding to the scatterer number(s) and absorber–scatterer distance(s) until the best possible fit is obtained. If the fit between calculated and observed EXAFS is not satisfactory, the elemental assignment of the scatterers is changed and/or an additional type of scatterer is added. A flow chart illustrating the overall procedure is given as Figure 1 of ref 2b.

The final fits on the different sets of Fourier-filtered Avl EXAFS are presented in Figure 7, and the calculated scatterer numbers and distances are recorded in Table I. The curve-fitting analysis began using the Mo–S and Mo–Fe distances and amplitudes previously obtained for Cpl. As expected, a reasonable fit was obtained using three waves on the Avl data from which the low-frequency component had been removed, while such a fit was less than satisfactory on the less tightly filtered Avl data. To investigate what was necessary to obtain a reasonable fit in the latter case, an extra oxygen or sulfur wave was added to account for the low-frequency component. The results in Table I indicate that if the low-frequency component were real, it would most likely correspond to an extremely short Mo–S distance. The best fit with oxygen parameters gave a *negative* number of oxygens, indicating that the phase of the low-frequency component is substantially different from that of a Mo–O interaction, and that there is still no evidence in the EXAFS for the presence of Mo–O bonds.

## Discussion and Conclusions

Although much of the preliminary Cpl, Avl, and FeMo-co data is relatively noisy, there exists a strong similarity in both edge and EXAFS spectra among all three cases. This spectral correspondence between three different samples under

**Table I.** Fitting Results on "Crystalline" Avl EXAFS Data<sup>a</sup>

Data	Minimization function value	S1		Fe		S2		X	
		Mo-S, Å	No.	Mo-Fe, Å	No.	Mo-S, Å	No.	Mo-X, Å	No.
Avl, low frequency removed	0.721	2.372	4.1	2.710	1.9	2.550	1.4		
Avl, low frequency kept in	1.302	2.354	3.5	2.729	1.7	2.465	1.5		
	1.249	2.354 <sup>b</sup>	3.5 <sup>b</sup>	2.729 <sup>b</sup>	1.7 <sup>b</sup>	2.465 <sup>b</sup>	1.5 <sup>b</sup>	2.043	0.5 O
	0.870	2.354 <sup>b</sup>	3.5 <sup>b</sup>	2.729 <sup>b</sup>	1.7 <sup>b</sup>	2.465 <sup>b</sup>	1.5 <sup>b</sup>	1.866	-1.1 O
	0.619	2.354 <sup>b</sup>	3.5 <sup>b</sup>	2.729 <sup>b</sup>	1.7 <sup>b</sup>	2.465 <sup>b</sup>	1.5 <sup>b</sup>	1.844	0.8 S
	0.578	2.363	4.0	2.721	1.8	2.505	1.2	1.846	0.8 S
Cpl	0.485	2.353	3.7	2.724	1.4	2.481	1.0		

<sup>a</sup> For all fits, the analysis range was 4–12.5 Å<sup>-1</sup> using *k*<sup>6</sup> weighting. <sup>b</sup> Value fixed during optimization.

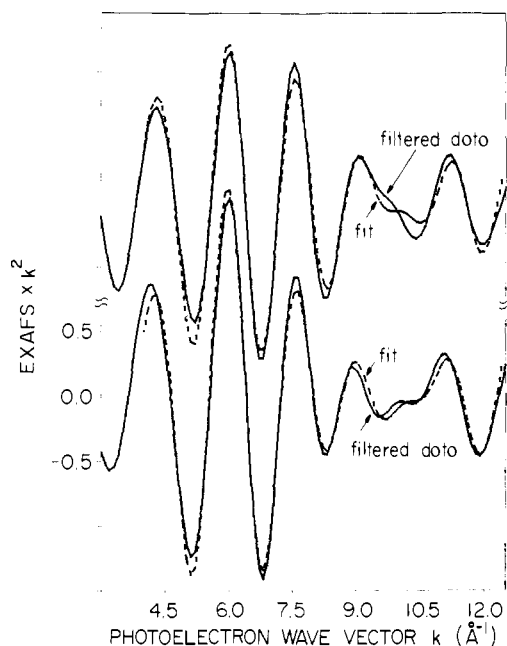


**Figure 7.** Fourier-filtered and curve-fitted Avl EXAFS. Top curves, (—) Avl EXAFS with low *R* peak removed, and (---) best three-wave fit. Bottom curves, (—) Avl EXAFS with low *R* peak included, and (---) best four-wave fit.

markedly different conditions—lyophilized Cpl, crystallized Avl, and FeMo-co in NMF solution—is the most important result of this initial investigation. The data reproduce for solvated systems the results previously obtained for lyophilized protein, and clearly indicate that lyophilization of this protein does not destroy the Mo environment. Furthermore, the data support the idea of a common and invariant Mo site structure in all nitrogenase Mo-Fe proteins, as suggested earlier by chemical results with the FeMo-co.<sup>4</sup>

The absorption edge spectra alone reveal some quite useful facts about this common Mo site. As we have previously discussed in detail,<sup>3</sup> the relatively low-energy position of the Mo K edge in the Cpl spectrum strongly indicates the existence of primarily sulfur ligation to Mo, and the similarity of the Avl and FeMo-co edges supports this conclusion for these cases as well. Such a conclusion is indirectly supported by the fact that mersalyl treatment of the Mo-Fe protein causes release of the Mo;<sup>12</sup> furthermore, similar treatment of the iron-molybdenum cofactor causes substantial changes in the optical spectrum.<sup>4</sup>

The second constraint imposed by the edge results is the absence of doubly bound oxygen (Mo=O) from the Mo site. Such Mo=O bonds have been shown to substantially enhance the intensity of the nominally forbidden 1s–4d transition(s). Thus, with one or two Mo=O, a shoulder appears on the absorption edge, while with three or four Mo=O bonds a separate peak is observed for the 1s–4d transition.<sup>8</sup> As Figure 3

clearly shows, the 1s–4d transition for nitrogenase Mo is virtually undetectable, and doubly bound oxygen can be excluded as a ligand in all three cases.

The lack of Mo=O is probably one of the characteristics of nitrogenase molybdenum which distinguishes it from the Mo in other enzymes. Most other known Mo enzymes can be viewed as oxo-transfer catalysts, and Mo-bound oxygen atoms might be involved in their catalytic mechanism.<sup>13</sup> Previously, it was shown that air oxidation of nitrogenase molybdenum produced a species with one or two doubly bound oxygens (as well as other undefined ligands).<sup>3</sup> It has recently been shown<sup>14</sup> that FeMo-co is only associated with nitrogenase and that previous reports<sup>15</sup> that the same cofactor is common to all molybdoenzymes were in error.<sup>14,16</sup> Acid-treated extracts of non-nitrogenase Mo proteins are unable to activate inactive Mo-Fe protein from *A. vinelandii* mutant strain UW45,<sup>14</sup> and acid-treated, highly purified Avl and Cpl do not activate crude extracts of the *N. crassa* nit-1 mutant.<sup>14,16</sup> However, it still appears that xanthine oxidase, nitrate reductase, aldehyde oxidase, and sulfite oxidase all share a common molybdenum cofactor.<sup>14,15,17</sup>

The curve-fitting results on the crystallized Avl EXAFS confirm the previous results using lyophilized Cpl spectra. A comparison of the best fit results of both analyses (Table I) reveals that the average deviation between comparable calculated Mo-X distances was 0.012 Å. The calculated scatterer numbers were also in good agreement; the slightly larger Avl values most likely reflect the fact that these data were collected at dry ice temperature rather than at room temperature. Although a fourth component was necessary to fit the Avl EXAFS, the physical origin and reproducibility of this feature are questionable.

It is clear at this point that a valid structural model for the Mo site of nitrogenase will necessarily involve two major features: (1) a set of three or four bound sulfur atoms with an average Mo-S distance of about 2.36 ± 0.02 Å, and (2) a set of two or three iron atoms at a distance of 2.72 ± 0.03 Å from the Mo. A less unambiguous result of the fitting calculations is the presence of one or two sulfurs with longer Mo-S bonds of about 2.49 Å. The expected error for this latter distance is difficult to assign, but in a wide range of fitting procedures this distance stayed within the range of 2.46–2.55 Å. The final component of the four-wave Avl fit, involving a chemically unreasonable Mo-S distance of 1.85 Å, is thought to be a low-frequency artifact of the background subtraction procedure, and further data collection is necessary to clarify this point.

EXAFS data itself provides no information about bond angles or the connectivity of the various scattering atoms. However, one can use the distance information supplied by EXAFS in combination with crystallographically determined bond lengths and known chemistry to make reasonable guesses about molecular structure. Such a procedure was used in the previous analysis of the Cpl EXAFS, and two possible types of Mo, Fe, S clusters were suggested as reasonable explanations

for the observed spectra. The new Avl and FeMo-co data essentially reproduce this earlier work, but under solvated rather than lyophilized conditions. Thus, it appears that the molybdenum site is very similar if not identical in all three systems. Further spectroscopic studies of nitrogenase and model compounds at liquid nitrogen temperatures should help reduce some of the current ambiguity about scatterer numbers, while solution studies of the steady-state nitrogenase system in the presence of substrates and inhibitors promise to yield information about the role of molybdenum in the catalytic mechanism.

**Acknowledgments.** We wish to thank Sebastian Doniach for numerous helpful discussions about the x-ray absorption spectroscopy analysis and for his continued encouragement. We thank Thomas Eccles for the computer programming of both data collection and data analysis packages and Deloria Jacobs for assistance with the AVI preparation. K.O.H. is a fellow of the Alfred P. Sloan Foundation and S.P.C. was an IBM Doctoral Fellow for 1976–1977. This work was supported by the National Science Foundation through Grant PCM-75-17105 and 76-24271 and by NIH Grant GM 22130. Synchrotron radiation time was provided through the Stanford Synchrotron Radiation Laboratory supported by NSF Grant DMR-07692-A02 in cooperation with the Stanford Linear Accelerator Center and the Department of Energy.

## References and Notes

- (1) (a) Stanford University; (b) Purdue University; (c) Charles F. Kettering Research Laboratory; (d) University of Wisconsin.
- (2) (a) For a recent review of nitrogenase research see W. H. Orme-Johnson and R. H. Sands in "Iron-Sulfur Proteins", Vol. 3, W. Lovenberg, Ed., Academic Press, New York, N.Y., 1977. (b) S. P. Cramer, K. O. Hodgson, E. I. Stiefel, and W. E. Newton, *J. Am. Chem. Soc.*, **100**, 2748 (1978), and references cited therein.
- (3) S. P. Cramer, K. O. Hodgson, W. O. Gillum, and L. E. Mortenson, *J. Am. Chem. Soc.*, **100**, 3398 (1978).
- (4) V. K. Shah and W. J. Brill, *Proc. Natl. Acad. Sci. U.S.A.*, **74**, 3249 (1977).
- (5) (a) W. A. Bulen and J. R. LeComte, *Proc. Natl. Acad. Sci. U.S.A.*, **56**, 979 (1966); (b) A. G. Gornall, C. J. Bardawill, and M. M. David, *J. Biol. Chem.*, **177**, 751 (1949); (c) L. J. Clark and J. H. Axley, *Anal. Chem.*, **27**, 2000 (1955); (d) R. E. Peterson, *ibid.*, **25**, 1337 (1953).
- (6) V. K. Shah and W. J. Brill, *Biochim. Biophys. Acta*, **305**, 445 (1973).
- (7) T. K. Eccles, Ph.D. Thesis, Stanford University, 1977.
- (8) S. P. Cramer, Ph.D. Thesis, Stanford University, 1977.
- (9) V. H. Hu, S. I. Chan, and G. S. Brown, *Proc. Natl. Acad. Sci. U.S.A.*, **74**, 3821 (1977).
- (10) R. G. Shulman, Y. Yafet, P. Eisenberger, and W. E. Blumberg, *Proc. Natl. Acad. Sci. U.S.A.*, **73**, 1384 (1976).
- (11) E. A. Stern, D. E. Sayers, and F. W. Lytle, *Phys. Rev. Sect. B*, **11**, 4836 (1975).
- (12) L. E. Mortenson, unpublished results.
- (13) P. W. Schneider, D. C. Bravard, J. W. McDonald, and W. E. Newton, *J. Am. Chem. Soc.*, **94**, 8640 (1972).
- (14) P. T. Pienkos, V. K. Shah, and W. J. Brill, *Proc. Natl. Acad. Sci. U.S.A.*, **74**, 5468 (1977).
- (15) A. Nason, K. Y. Lee, S. S. Pan, P. A. Ketchum, A. Lamberti, and J. DeVries, *Proc. Natl. Acad. Sci. U.S.A.*, **68**, 3242 (1971).
- (16) B. B. Elliott, L. E. Mortenson, and E. I. Stiefel, unpublished results.
- (17) J. L. Johnson, H. P. Jones and K. V. Rajagopalan, *J. Biol. Chem.*, **252**, 4994 (1977).

## The Photochemistry of 2-Vinylstilbenes. 2.<sup>1</sup> Photoreactions of 2-Vinyl- and 2-Propenylstilbene and of Ortho-Substitution Products

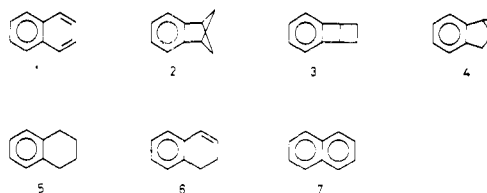
M. Sindler-Kulyk and W. H. Laarhoven\*

Contribution from the Department of Organic Chemistry, Catholic University, Toernooiveld, Nijmegen, The Netherlands. Received September 7, 1977

**Abstract:** Irradiation of 2-vinylstilbene **19** results in the formation of *exo*-5-phenylbicyclo[2.1.1]hex-2-ene (*exo*-**21**) as the main product (70%). As contrasted with the results with *o*-divinylbenzene no benzobicyclo[3.1.0]hex-2-ene derivative (**23**) is formed. Irradiation of 2-propenylstilbene (**20**) gives rise to both types of products, viz., 30% *endo*-5-methyl-*exo*-6-phenylbicyclo[2.1.1]hex-2-ene (**27**) and 10% *exo*-4-methyl-*endo*-6-phenylbicyclo[3.1.0]hex-2-ene (**28**). Irradiation of 2-vinylstilbenes substituted at one ortho position of the  $\beta$  ring gives a qualitatively similar result as the parent compound; the main product is an *exo*-6-phenylbicyclo[2.1.1]hex-2-ene derivative. On introduction of an ortho substituent in the  $\alpha$  ring a similar product is obtained, but an *endo*-6-phenylbicyclo[3.1.0]hex-2-ene derivative is isolated as a second product. 2-Vinylstilbenes having two ortho substituents in the  $\beta$  ring give neither of these photoproducts. The different behavior has been explained by the supposition that the photoproducts mainly arise from the *cis* isomer of the starting compounds, and that distinct products originate from different conformations of the *cis* isomers. The supposition has been supported by stereochemical considerations, calculation of Mulliken overlap populations, and NMR data. Most probably the photoreactions occur from the S<sub>1</sub> states. The bicyclo[2.1.1]hexene derivatives are formed by a radical reaction whereas the bicyclo[3.1.0]hexenes may arise from a concerted process. Only when the former reaction is not much faster than the latter are both types of products found.

### Introduction

Some years ago Pomerantz<sup>2</sup> and Meinwald and Mazzocchi<sup>3</sup> reported for the first time the photochemical behavior of *o*-divinylbenzene (**1**), a hexatriene with one double bond of reduced bond order because of its inclusion in an aromatic ring. They envisaged that the replacement of the central double bond by a benzene ring should cause head-to-tail cycloaddition between the vinyl groups to give benzobicyclo[2.1.1]hexane (**2**), as observed with 1,5-hexadienes.<sup>4</sup> However, the irradiation of a dilute solution of **1** in ether or pentane yielded neither **2** nor the head-to-head cycloaddition product **3**, but rather benzo-



bicyclo[3.1.0]hexene (**4**) in 30% yield, a product analogous to one of the photoproducts of 1,3,5-hexatriene.<sup>5</sup> Furthermore, traces of tetralin (**5**), 1,2-dihydronaphthalene (**6**), and naphthalene (**7**) have been found.<sup>6</sup> The formation of **4** requires the